

NOVEMBER 29 2021

# Simultaneous velocity and concentration profiling of nuclear waste suspensions in pipe-flow, using ultrasonic Doppler and backscatter analysis **FREE**

Serish Tanya Hussain; Jeffrey Peakall; Martyn Barnes; Timothy Hunter



*Proc. Mtgs. Acoust* 45, 070002 (2021)

<https://doi.org/10.1121/2.0001525>



View  
Online



Export  
Citation

CrossMark



**ASA**

Advance your science and career as a member of the  
**Acoustical Society of America**

**LEARN MORE**

## 181st Meeting of the Acoustical Society of America

Seattle, Washington

29 November - 3 December 2021

### Underwater Acoustics: Paper 2pUW16

# Simultaneous velocity and concentration profiling of nuclear waste suspensions in pipe-flow, using ultrasonic Doppler and backscatter analysis

**Serish Tanya Hussain**

*Department of Chemical and Process Engineering, University of Leeds School of Chemical and Process Engineering, Leeds, West Yorkshire, LS2 9JT, UNITED KINGDOM; pm14sth@leeds.ac.uk*

**Jeffrey Peakall**

*University of Leeds School of Earth and Environment, Leeds, West Yorkshire, LS2 9JT, UNITED KINGDOM; J.Peakall@leeds.ac.uk*

**Martyn Barnes**

*Sellafield Ltd, Seascale, Cumbria, CA20 1PG, UNITED KINGDOM; martyn.g.barnes@sellafieldsites.com*

**Timothy Hunter**

*University of Leeds School of Chemical and Process Engineering, Leeds, West Yorkshire, LS2 9JT, UNITED KINGDOM; t.n.hunter@leeds.ac.uk*

Complex magnox ponds at Sellafield retain hydroxide-based sludge with unknown physicochemical properties where the sludge is a corroded form of magnesium-based fuel cladding. Long term storage and open-air aqueous conditions have been major contributors to corrosion and now the waste requires transportation to interim storage using engineered pipelines. Remote in situ characterization of sludge was achieved using a non-invasive ultrasonic velocity profiler (UVP) which monitored suspensions in a bespoke pipe-loop designed to mimic flows encountered in the nuclear industry. Spherical glass particles with two size distributions of known acoustic behavior were analyzed to extract raw velocity and echo amplitude for velocity and acoustic profiling which provided insight into the effect of particle size and concentration on attenuation. Four 4 MHz frequency transducers were mounted in-line on engineered pipelines, 90° and 135° to flow on horizontal and vertical pipe sections where acoustic profiles were compared to select the most efficient pipe arrangement. When comparing, the horizontal pipe section was found to enhance attenuation producing higher coefficient values, likely caused by suspension segregation. Simultaneous velocity profile measurement was achieved where profiles were as expected for highly turbulent flow. Moving forward, complex non-defined nuclear simulants will be analyzed to investigate the UVP's limitations.

## 1. INTRODUCTION

The online characterization of suspensions, whether it be the analysis of concentration, size, or flow behavior, can be a complex process. This is even more so in the nuclear industry as the risk of radiation exposure or contamination limits the number of techniques that can be used. Specifically, there are numerous nuclear waste suspensions and sludges stored in various ponds, siloes and tanks at reactor sites worldwide that require safe and remote characterization as part of waste transfer and processing operations<sup>1</sup>, such as at Sellafield, one of Europe's largest reprocessing facilities. Online monitoring of suspension concentrations is often achieved in similar industries using  $\gamma$ -ray densitometers or Coriolis meters<sup>2</sup> although they can be very expensive and challenging to retrofit onto existing pipelines. Additionally, they offer no potential to profile suspensions to investigate segregation, and also do not allow for the extraction of other critical information, such as suspension particle size. Ultrasonic profilers, however, do offer the ability to extract simultaneous concentration and flow data from suspensions, and also indicate particle size from the scattering-attenuation relationship<sup>3,4,5</sup>. They can also be relatively easily installed in many systems using non-contacting clamp-on mounting blocks. The purpose of this investigation is to understand the behavior of suspensions in engineered pipelines, and their online characterization with ultrasonic meters, where results can be applied to aid the transfer and processing of nuclear waste suspensions<sup>6</sup>. Engineered pipelines are used across industries, especially in the wastewater treatment sector and oil and gas, so a new streamlined process for analysis and characterization could be adapted for many applications<sup>7</sup>. Within the nuclear industry, remote techniques are particularly valuable as the equipment is not in direct contact with the suspension which limits the risk of contamination<sup>8</sup>.

When selecting a remote characterization technique, there are several options that could be used, however, ultrasonic acoustics are potentially the most practical and applicable technique, as it has been utilized frequently in marine surveying, where ultrasonic transducers underwater were used to detect aquatic marine life on the seabed<sup>9</sup>. Here, acoustic backscatter systems (ABS) are used where a single probe or probe array acts both to generate the ultrasound and detect the echo signal, allowing for depth profiles. In the current work, a commercial ultrasonic velocity profiler (UVP) was used in backscatter mode to enable attenuation measurements from the voltage response. Similar UVP systems have been previously used in well mixed tanks to measure the attenuation of various suspensions, where probes were mounted onto the outside of tank walls, enabling analysis in non-contact configurations<sup>5,10</sup>.

Here, a UVP was used to monitor suspension flows in a bespoke pipe-loop designed to mimic flows encountered in the transferring of nuclear wastes. The pipe-loop was manufactured with both vertical and horizontal test sections, and integrated transducers were mounted onto the outside of the pipeline in each section, where the pipe orientation with the most efficient acoustic profile data was selected for velocity profiling. As the UVP enables simultaneous collection of velocity data using the Doppler shift, probes were mounted at two angles (90° and 135°) for optimal collection of attenuation and velocity data respectively. For the initial rig validation reported here, two different sizes of glass bead dispersions were used, as their scattering-attenuation is well understood theoretically, while calibration data exists on their attenuation coefficients<sup>3,5</sup>. Difference in particle size provided deeper insight into the change of acoustic behavior of slurries in pipelines<sup>11</sup>, while the simultaneous collection of velocity and echo amplitude data from the UVP allows for complex real-time characterization of sediment transport, in a safe, industrially deployable unit.

## 2. THEORY

### A. PIPE FLOW ENTRY CALCULATIONS

The experimental flowrate for the studied conditions was calculated by measuring the volume of water extracted from the drainage point in the pipe loop over a time period of five seconds. The measured flow rate was used to establish the mean flow velocity by using the area of the pipe, where the internal pipe diameter was 0.025 m. The Reynolds number,  $Re$ , corresponding to the flow rate was calculated from Eq. (1)<sup>12</sup> using the kinematic viscosity,  $\nu$  ( $\text{m}^2 \cdot \text{s}^{-1}$ ), pipe diameter,  $D$  (m), and the flow velocity,  $U_{ave}$  ( $\text{m} \cdot \text{s}^{-1}$ ). The kinematic viscosity of water at room temperature<sup>12</sup> 20 °C,  $\nu = 10^{-6} \text{ m}^2 \cdot \text{s}^{-1}$  was used, while the contribution from the particles on the viscosity were negated, because of the small concentrations used (0.46 to 4.97 vol %)<sup>13</sup>.

$$Re = U_{ave} \frac{D}{\nu} \quad (1)$$

The minimum required ratio of entry length, to pipe diameter ( $L/D$ ) for the pipe-loop was calculated<sup>14</sup> to ensure the flow was fully developed before the measuring location. Two methods for calculating the ratio of entry length were used for validation, one method used the Reynolds number whilst the other utilized the roughness coefficient of PVC pipes ( $\sim 1.5 \times 10^{-6}$  m)<sup>15</sup>. The minimum length to diameter ( $L/D$ ) ratio was first calculated in Eq. (2), using the Reynolds number<sup>14,16</sup>, which was converted to the minimum entry length using the known diameter,  $D = 0.025$  (m)<sup>14</sup>. The  $L/D$  ratio and minimum entry length for various flowrates achievable with the pump system used are shown in Table 1, giving a range from 0.47 to 0.60 m, which was significantly smaller than the actual entry lengths for both horizontal (1.3 m) and vertical (2.1 m) pipe sections (see Section 3-B). Therefore, flow was fully developed at the points of analysis in the vertical and horizontal probe holders.

$$\frac{L}{D} (\text{method 1}) = 4.4Re^{\frac{1}{6}} \quad (2)$$

**Table 1. Calculation of minimum entry length requirements using method 1 (Eq. (2)).**

Speed (RPM)	Flow rate (L/s)	Flow Rate (m <sup>3</sup> /s)	Flow Velocity $U_{ave}$ (m/s)	Reynolds Number, Re	Minimum Length to Diameter, $L/D$ (method 1)	Minimum Entry Length, $L$ (m)
150	0.12	0.00012	0.23	5857	18.68	0.47
300	0.16	0.00016	0.33	8149	19.74	0.49
900	0.43	0.00043	0.88	22002	23.29	0.58
1050	0.50	0.00050	1.03	25669	23.90	0.60

Entry length was also calculated utilizing a second method as a validation step by using the Darcy friction factor<sup>17</sup>,  $f$ . The friction factor was calculated in Eq. (3) using the Reynolds number, Re from Table 1, as well as the roughness coefficient,  $\varepsilon$  (m) and the pipe diameter  $D$  (m)<sup>14</sup>. The entry length was consequently calculated using the friction factor values found using Eq. (3)<sup>18</sup>. All entry lengths shown in Table 2 range from 0.37 to 0.53 m, which is similar to method 1, all be it slightly lower in length estimations. Nevertheless, by calculating the entry length using two independent methods, it was confirmed that flow was fully developed before analysis.

$$f^{-\frac{1}{2}} = -1.8 \log \left[ \frac{6.9}{Re} + \left( \frac{\varepsilon}{3.7D} \right)^{1.11} \right], \quad \frac{L}{D} (\text{method 2}) = \frac{0.5}{f} + \frac{5}{f^2} \quad (3)$$

**Table 2. Reynolds number and friction factor calculations for the second methodology (Eq. (3)) to determine the minimum entry length requirements.**

Reynolds Number, Re	Friction factor $f^{-0.5}$	Friction factor $f$	Minimum Length to Diameter $L/D$ (method 2)	Minimum entry Length, $L$
5857	5.27	0.036	14.83	0.37
8149	5.53	0.033	16.17	0.40
22002	6.29	0.025	20.61	0.52
25669	6.41	0.024	21.34	0.53

## B. ACOUSTIC THEORY

The ultrasonic velocity profiler (UVP) analyzes suspensions by emitting pulsed signals through the pipe and detecting any reflected signals. Echo amplitude data is extracted from the UVP where the amplitude shows the attenuation of sound as the sound signal propagates through the suspension. The ratio of attenuation to detection of sound allows the UVP to differentiate between suspensions of varying concentrations and particle size distributions. Echo amplitude,  $E(r)$ , is converted to voltage in Eq. (4), using the gain function,  $g(r)$ , which is selected depending on the amplification required for the signal<sup>19</sup>.

$$V(r) = \frac{3.052 \times 10^{-4} E(r)}{g(r)} \quad (4)$$

In Eq. (5), the voltage is a function of concentration,  $M$  ( $\text{kg.m}^{-3}$ ), attenuation due to solid and water,  $\alpha_s$  ( $\text{m}^{-1}$ ),  $\alpha_w$  ( $\text{m}^{-1}$ ), as well as the transducer constant,  $k_t$  ( $\text{V.m}^{1.5}$ ) and the backscatter coefficient  $k_s$  ( $\text{m.kg}^{0.5}$ )<sup>20</sup>. The nearfield correction factor in Eq. (6) is a function of the distance  $r$  (m), transducer active radius  $a_t$  (m) and wavelength  $\lambda$  (m), where the wavelength is calculated using the speed of sound in water (1480 m/s) and transducer frequency (4 MHz).

$$V = \frac{k_s k_t}{\psi r} M^{1/2} e^{-2r(\alpha_w + \alpha_s)} \quad (5)$$

$$\psi = \frac{1 + 1.35 \left( \frac{r}{\frac{\pi a_t^2}{\lambda}} \right) + \left( 2.5 \left( \frac{r}{\frac{\pi a_t^2}{\lambda}} \right) \right)^{3.2}}{1.35 \left( \frac{r}{\frac{\pi a_t^2}{\lambda}} \right) + \left( 2.5 \left( \frac{r}{\frac{\pi a_t^2}{\lambda}} \right) \right)^{3.2}} \quad (6)$$

The speed of sound in suspensions can be calculated using the density  $\rho$  ( $\text{kg.m}^{-3}$ ) and compressibility  $k$  ( $\text{m}^2.\text{N}^{-1}$ ) of the suspension, as originally devised by Urick<sup>21</sup>, which are both additive properties. Hence for Eq. (7), the density and compressibility are calculated as volume fractions of the suspension's components. In Eq. (7),  $\phi$  indicates the volume fraction of the sediment, whilst the subscripts  $s$  and  $w$ , indicate values for sediment and water, respectively<sup>21</sup>.

$$c = \frac{1}{\sqrt{\rho k}}, \quad \rho = \rho_w \phi + \rho_s (1 - \phi), \quad k = k_w \phi + k_s (1 - \phi) \quad (7)$$

**Table 3. Speed of sound calculations for silica glass bead suspensions**

Concentration, $M$ ( $\text{kg.m}^{-3}$ )	Volume ( $\text{m}^3$ )	Volume (%)	Density, $\rho$ ( $\text{kg.m}^{-3}$ )	Compressibility, $k$ ( $\text{m}^2.\text{N}^{-1}$ )	Speed of sound, $c$ (m/s)	$\Delta c/ c_0$
11.9	0.0002	0.46	1004	4.56E-10	1478	-0.15
35.7	0.0006	1.35	1019	4.52E-10	1474	-0.44
47.6	0.0008	1.80	1026	4.50E-10	1472	-0.57
59.5	0.0010	2.24	1033	4.48E-10	1470	-0.70
83.3	0.0014	3.11	1047	4.44E-10	1466	-0.95
107.5	0.0017	3.97	1061	4.41E-10	1463	-1.18

The speed of sound was calculated for glass test materials, as shown above in Table 3. While the testing program used two different sizes of glass (see Section 3) their speed of sound is identical, as the Urlick equations do not consider particle size<sup>21</sup>. The density of silica dioxide (2500 kg.m<sup>-3</sup>) was used as the silica glass beads are composed of ~75% silica dioxide<sup>22</sup>. Compressibility was calculated by taking the inverse of bulk modulus, wherein the bulk modulus of silica dioxide (36.9 GPa) was used. Table 3 shows that an increase in density led to a decrease in the speed of sound.

A logarithmic function of the voltage, called the  $G$ -function, was used to compare attenuation of profiles, wherein it is calculated using the suspension concentration,  $M$  (kg.m<sup>-3</sup>), attenuation due to solid and water,  $\alpha_s$  (m<sup>-1</sup>),  $\alpha_w$  (m<sup>-1</sup>), as well as the transducer constant,  $k_t$  (V.m<sup>1.5</sup>) and the backscatter coefficient  $k_s$  (m.kg<sup>0.5</sup>)<sup>20</sup>. The  $G$ -function utilizes the nearfield coefficient<sup>23</sup>,  $\psi$ , and distance from transducer,  $r$  (m) to calculate the logarithmic voltage. The acoustic model below was outlined using previous literature<sup>19,24</sup>.

$$G = \ln(\psi r V) = \ln(k_s k_t) + \frac{1}{2} \ln M - 2r(\alpha_w + \alpha_s) \quad (8)$$

The attenuation constant ( $\zeta$ , in m<sup>2</sup>.kg<sup>-1</sup>) was calculated using the gradient found when plotting the logarithmic  $G$ -function vs  $r$ , distance from transducer (m). This attenuation constant changed with concentration, particle size and shape<sup>25</sup>. The sedimentation attenuation coefficient was calculated using Eq. (9).

$$\xi_s = -\frac{1}{2} \frac{\partial^2 G}{\partial M \partial r} = -\frac{1}{2} \frac{\partial}{\partial M} \left[ \frac{\partial}{\partial r} [\ln(\psi r V)] \right] \quad (9)$$

### 3. EXPERIMENTAL METHODS

#### A. MATERIALS

For the testing program, spherical silica glass particles in two sizes were used (Honite, Guyson Ltd)<sup>11</sup> as their acoustic scattering profiles have been well researched and calibration attenuation values are available for well mixed systems<sup>3</sup>. A Mastersizer 3000 (Malvern Panalytical) was used to determine the size of the two silica glass beads where the cumulative particle size distributions were extracted and are shown for both species in Fig. 1. Median ( $d_{50}$ ) values were measured to be 38 and 78  $\mu\text{m}$  for the two sizes, labelled ‘small glass’ and ‘large glass’ respectively for simplicity throughout.

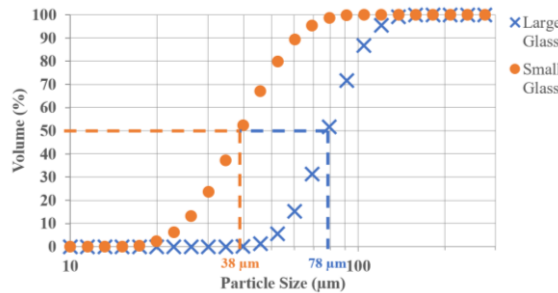


**Figure 1. Cumulative particle size distribution of small ( $d_{50}$  - 38  $\mu\text{m}$ ) and large ( $d_{50}$  - 78  $\mu\text{m}$ ) silica glass beads.**

A desktop scanning electron microscope (TM3030Plus, Hitachi) was utilized to produce micrographs of both glass sizes to confirm particle morphology (Fig. 2). The spherical shape of the particles can be seen for both glass bead sizes, where average sizes measured from the images were comparable to the cumulative particle size distribution data in Fig. 1. It is also noted that for Fig. 2a, the particle size distribution appeared visibly more varied with a few non-spherical particles, whilst the larger glass bead distribution was more uniform.

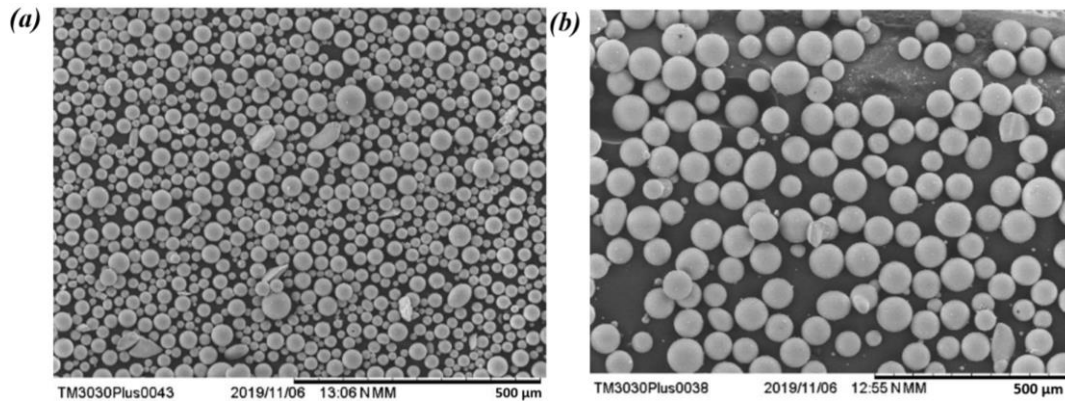


**Fig. 2. SEM images of (a) small silica glass beads and (b) large silica glass beads.**

## B. PIPE LOOP

An engineered pipe loop was constructed using unplasticized polyvinyl chloride piping<sup>26</sup>, with clear sections for visual observation and an inner diameter of 25 mm (30 mm outer). Importantly, the rig was constructed to include both horizontal and downward facing vertical test sections, as shown schematically in Fig. 3, along with the associated pump and mixing tank. Selection of either vertical or horizontal test sections is achieved through a three-way valve which allowed investigations into the effect of pipe orientation on the quality of data collection by the ultrasonic profiler. The direction of flow is also indicated in Fig. 3 by arrows, which allow the reader to visualize suspension movement through the pipe loop.

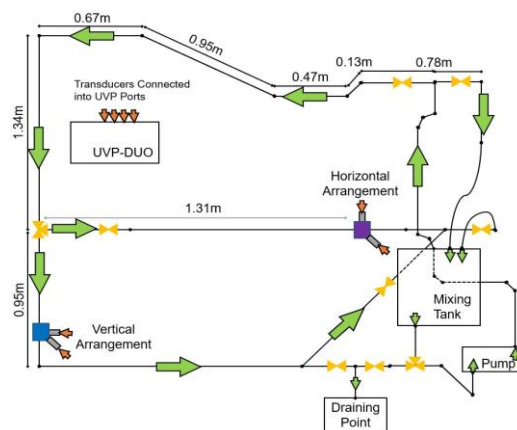


**Figure 3. Schematic of pipe loop with flow direction.**

The location of the ultrasonic transducers is shown in Fig. 3 by the blue and purple boxes, which indicate custom probe holders for the vertical and horizontal pipe orientations respectively, where two transducers were mounted in both arrangements: one at  $90^\circ$  and  $135^\circ$ . A schematic of the custom probe holders is shown in Fig. 4. Four 4 MHz transducers were used on this pipeline and each transducer was connected to an individual port on the UVP. The probe holders were designed so that the probe face was flush to a thin section of the holder that was undrilled, which then was fitted flush to the pipe itself. This arrangement helped mitigate the effects of pipe curvature, where audio gel was also added to help ultrasonic conduction between the probe, holder, and the pipe. The probes at  $90^\circ$  were used to measure sediment attenuation and thus produce concentration calibrations, while those at  $135^\circ$  to the flow were used to measure velocity profiles from the Doppler signal.

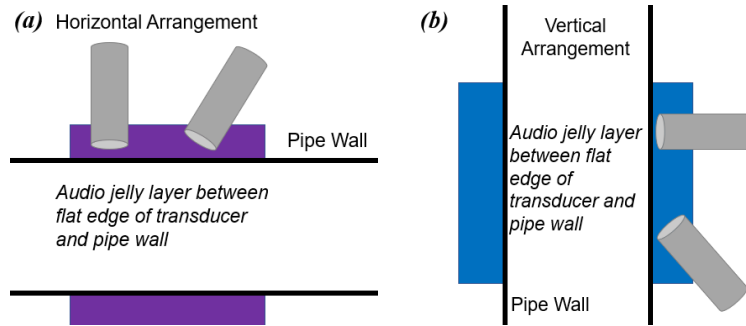


**Figure 4. (a) Horizontal mounting ports and (b) Vertical mounting ports for ultrasonic probes.**

For the experimental runs, glass bead powders were suspended in the mixing tank using an overhead impeller at a rate of 800 rpm (and a mixing diameter of 80 mm) to create a homogeneous suspension. Once all material was homogenized, the pump was used to circulate the suspension around the loop and across the horizontal or vertical testing section. The suspension was circulated for five minutes to ensure even distribution through the pipe before analysis. The flow rate of the pump was maintained at 0.5 L/s ( $Re = 25,669$ ) for all reported data, which was high enough to ensure all material was well suspended. It is noted that the actual entry lengths for the vertical and horizontal sections were 1.3 m and 2.1 m respectively, and so more than twice the calculated minimum entry lengths (see Tables 1 & 2).

Acoustic attenuation measurements of the suspensions were made using a UVP-DUO commercial UVP system (Met-flow SA, Switzerland) utilizing 4 MHz transducers. The system allows multiple transducers of the same frequency to be measured simultaneously, where a small delay was implemented between each transducer to ensure no overlap of signal<sup>27</sup>. Data was gathered separately for the probes in vertical and horizontal arrangements, where for each suspension concentration, the total measurement time was 62 seconds, comprising of 1023 individual profiles with a time period of 63 ms each. Suspension concentrations of 11.9–107.14 g/L were investigated for both glass species, as it has been previously shown that this range was suitable for accurately measuring their attenuation coefficients in a mixing tank using the  $G$ -function method<sup>3,5</sup>.

## 4. RESULTS AND DISCUSSION

### A. ACOUSTIC PROFILES

The acoustic profiles were analyzed as distance dependent  $G$ -function values, which were calculated from the return voltage using Eq. (4)<sup>19,28</sup>. The  $G$ -function profiles were utilized as an intermediate function to extract the sedimentation attenuation coefficient, which can be directly compared to values found in literature to determine the accuracy of the experiment<sup>19</sup>.

#### I. SMALL GLASS BEADS

Fig. 5(a) show the  $G$ -function profiles for the small glass bead suspensions travelling through a horizontal pipe arrangement. The estimated inner and outer pipe walls are indicated with the vertical lines in (a). The sound signal travels initially through a thin layer of the probe holder before penetrating through the pipe wall, where a layer of audio gel is placed between the transducer face and pipe wall to promote sound conduction. The noisy profile in the first ~0.005–0.009 m is attributed to internal reflections in the probe holder and pipe wall. The speed of sound through solid uPVC pipe wall<sup>29</sup> is ~2300 m/s however, the input for the UVP uses the speed of sound in water (1480 m/s) which leads to some ambiguity in where the pipe interfaces. Inside from the pipe wall, the profile is still noticeably noisy within the first 0.012 m, due to the complex near field interference from the ultrasonic transducers, and potentially suspension segregation in the pipeline. The increase in signal at 0.034 m is attributed to reflections at the back of the pipe wall, by extrapolating, the inner pipe wall is assumed to be at 0.009 m by using the actual inner pipe diameter of 0.025 m. It is also noted that the estimated speed of sound calculated for silica glass beads using the Urick equation (Table 3) indicate that the highest concentration produces a speed of sound of 1463 m/s, which is only 1.2% lower than water, and therefore would make a negligible difference on the echo distance estimations within the pipe.

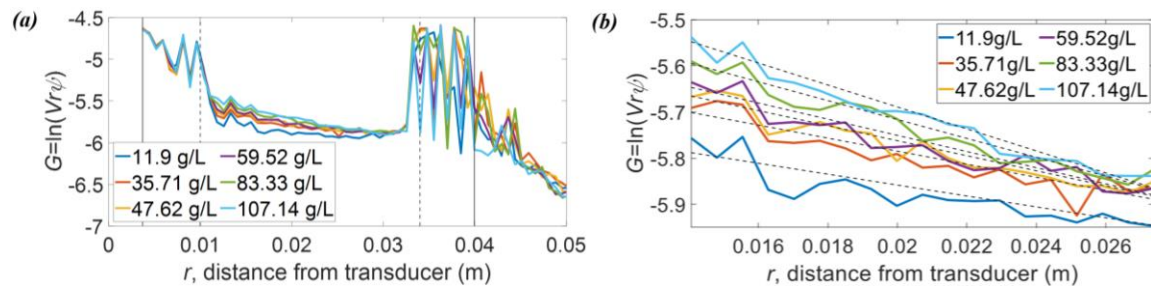


**Figure 5.** (a) *G*-function versus distance for small glass beads at varying concentrations in a horizontal arrangement and (b) Isolation of the linear region in (a). Vertical lines in (a) indicate estimated pipe boundaries and dashed lines in (b) are linear fits of the profiles.

To use the profile data more accurately for calibration purposes, a section between 0.014-0.028 m was selected to take the linear gradient ( $dG/dr$ ) values, as this zone gave consistent profiles outside of the nearfield region, but was before scattering interference from the far inner pipe wall. The profiles in this region are expanded in Fig. 5(b), as well as giving the decay trendlines. The profiles are approximately linear in this region (as would be expected for a largely constant concentration, from Eq (8-9)), although there is some degree of elevated noise in the averaged signal. The relatively low signal to noise ratio may indicate that the horizontal pipe orientation enhances suspension segregation in the pipe<sup>25</sup>, the smaller glass beads also have a limited backscatter response due to the decreased particle size, therefore, the noise in the profiles can also be attributed to the limitations of the UVP when analyzing a limited backscatter response. Nevertheless, sedimentation attenuation gradients extracted by the dashed lines indicated the higher particle concentrations lead to increased attenuation, from increased  $dG/dr$  values which is the change expected.

Fig. 6(a) similarly shows the acoustic profiles for small glass bead suspensions travelling through a vertical pipe arrangement, while again Fig. 6(b) presents a highlighted region used to extract the linear attenuation profiles for calibration. As with the horizontal arrangement, signals from the initial 0.005-0.008 m region are ignored, as they are within the pipe wall, where there is additional signal noise within the first 0.012 m from nearfield interference. However, it is noted that the profiles are less noisy than from the horizontal section (as evident in Fig. 6(b)). As there would not be any gravitational segregation across the pipe in the vertical arrangement, the improved signal to noise ratio further indicates that suspension segregation within the horizontal pipe led to a noisier profile. Interestingly, both pipe orientation profiles have a similar range of *G*-function values (approximately -5.5 to -6 in the suspension region) which shows that the signal strength of the transducers was consistent for both pipe orientations, as it is dominated by the relatively low backscatter from the smaller glass particles.

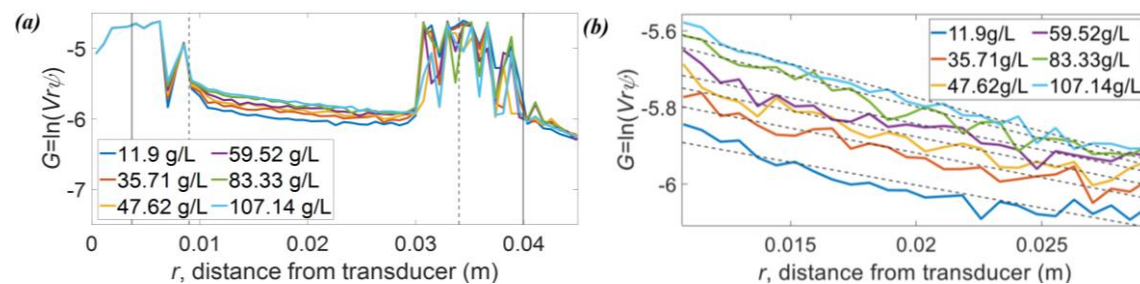


**Figure 6.** (a) *G*-function versus distance for small glass beads at varying concentrations in a vertical arrangement and (b) Isolation of the linear region in (a). Vertical lines in (a) indicate estimated pipe boundaries and dashed lines in (b) are linear fits of the profiles.

## II. LARGE GLASS BEADS

The acoustic profiles extracted from large glass bead suspensions travelling through the horizontal and vertical pipe arrangements are shown in Fig. 7 and 8 respectively. The same general features are present, as with the smaller glass, with the profiles from the first 0.012 m being ignored, due to the internal reflections from the pipe wall and nearfield interference from the initial suspension zone. Again, the level of signal noise from the averaged profiles was higher for the horizontal arrangement. Here, it was especially evident with the lowest 11.9 g/L concentration, where the delay within the suspension deviated from a linear trend expected from a homogeneous concentration, inferring even higher levels of segregation due to the larger particle size. Indeed, the deviation in the expected linear signal

decay meant that a smaller region in the far side of the pipe was taken to obtain average  $dG/dr$  values for the horizontal arrangement (from 0.018–0.029 m) as shown in Fig. 7(b). For the vertical arrangement, a larger section from 0.01–0.029 m (Fig. 8(b)) was taken to gain average linear gradient values for the calculation of attenuation coefficients.

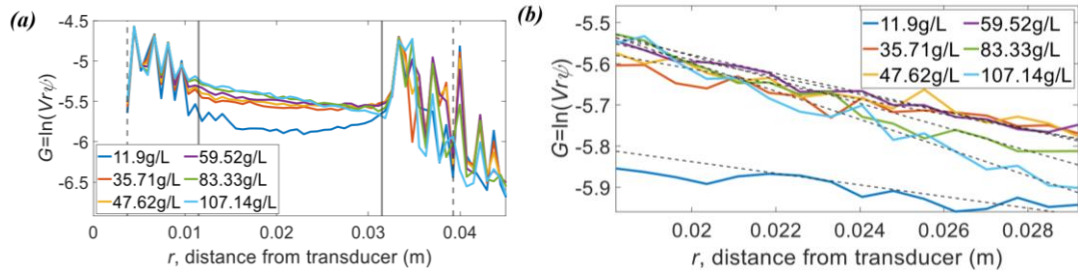


**Figure 7.** *G*-function versus distance for large glass beads at varying concentrations in a horizontal arrangement and (b) Isolation of the linear region in (a). Vertical lines in (a) indicate estimated pipe boundaries and dashed lines in (b) are linear fits of the profiles.

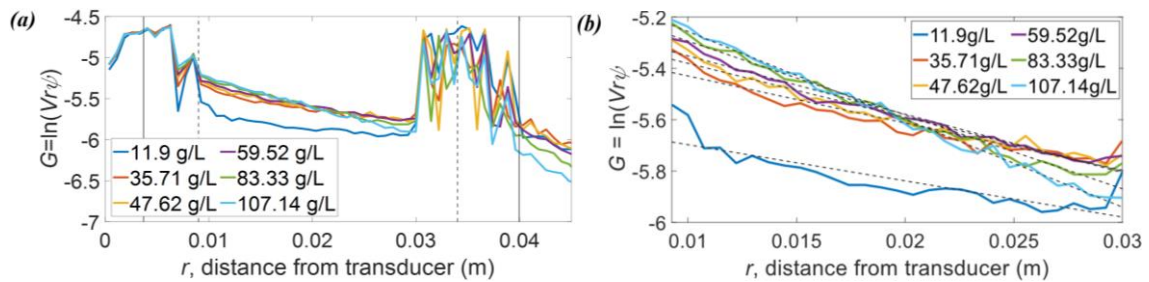


**Figure 8.** *G*-function versus distance for large glass beads at varying concentrations in a vertical arrangement and (b) Isolation of the linear region in (a). Vertical lines in (a) indicate estimated pipe boundaries and dashed lines in (b) are linear fits of the profiles.

### III. COMPARISON OF SEDIMENTATION ATTENUATION COEFFICIENTS

The isolated linear regions shown in Fig. 5(b), 6(b), 7(b) and 8(b) were utilized to extract the gradients ( $dG/dr$ ) at each concentration. These gradients were then plotted against their corresponding concentration values to produce an attenuation profile, where Fig. 9(a) and (b) present the profiles for the small glass and large glass suspensions respectively (with horizontal and vertical arrangements being directly compared). The dashed linear trendlines in these figures are used to directly calculate the concentration independent attenuation coefficients (using Eq. (9)) where for both particle sizes, the vertical pipe arrangement attenuates less (gradient versus concentration is less steep). It is assumed that the higher attenuation in the horizontal arrangement may be again from suspension segregation. As the isolated linear suspension region was towards the bottom of the horizontal pipe, any segregation may increase the relative concentrations as they become depleted from the top of the pipe. Such an increase in relative concentration would lead to higher relative attenuation, as the actual concentrations in the measurement zone may be greater than assumed from the added particle levels. Interestingly also, for the small glass, actual  $dG/dr$  values for both arrangements are relatively similar at lower concentrations, implying a similar backscatter profile, where differences are attenuated as concentration is increased. For the large glass, however,  $dG/dr$  values are very different for both arrangements across the entire concentration range. Specifically at low concentrations, it is hypothesized that the level of segregation with the large glass is great enough that the backscatter is considerably affected by the depletion of the suspension. Given that these correlations require a region of homogenous concentration to accurately estimate suspension attenuation, it is likely therefore that measured attenuation values may be inaccurate.

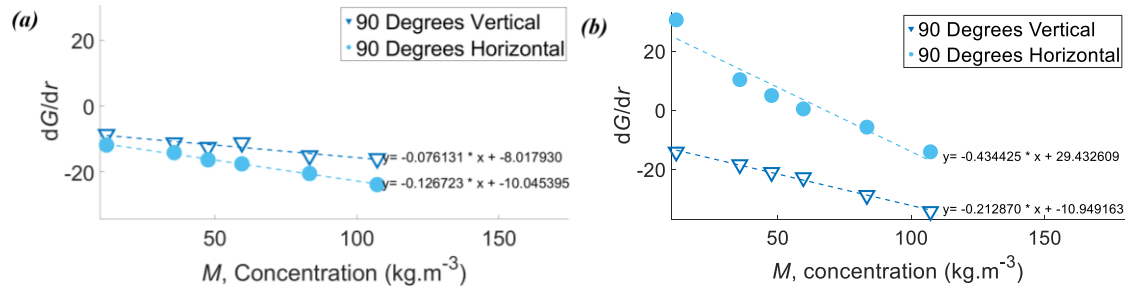


**Figure 9.** Change in G-function with distance ( $dG/dr$ ) for suspensions with a concentration range between 11 and 110 g/L for probes mounted at 90° in vertical and horizontal arrangements using (a) small glass beads suspensions and (b) large glass bead suspensions.

To directly compare concentration independent attenuation coefficients, values were calculated from the gradients in Fig. 9(a) and (b) using Eq. (9), as shown in Fig. 10. Calibration values extracted from previous literature<sup>3</sup> using the same particle species in a homogenous mixing tank are also shown for direct comparison, where error bars for all systems are calculated from the array of echo data across the 1023 profiles. The coefficient values for the horizontal arrangement in both particle suspensions are almost double those of the vertical arrangement (which again is assumed to be due to segregation in the pipe leading to an increase in attenuation) where values from the vertical arrangement are closer to the calibration data. This correlation is particularly true for the large glass beads, where the overestimation of the horizontal arrangement is considerable. It is also noted that, in line with theoretical expectations<sup>3,5,19,24</sup>, attenuation values for the larger particles are higher, due to the enhanced scattering from the larger particle cross-sections. Hence, it is evident that transducers mounted on a vertical pipe arrangement are able to produce accurate acoustic profiles and attenuation coefficients, and thus it is recommended that any future industrial monitoring applications should use vertical mounting configurations.

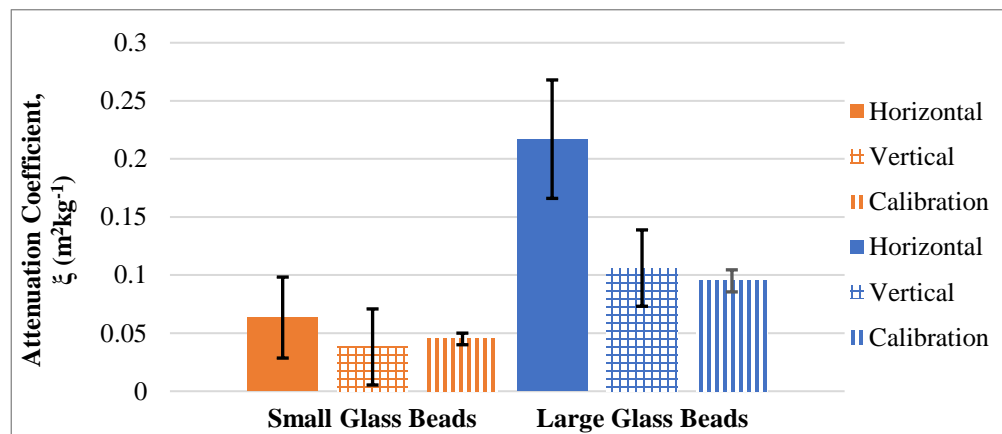


**Figure 10.** Attenuation coefficients from both pipe loop arrangements and particle sizes, in comparison to calibration data<sup>3</sup>. Error bars calculated using the standard deviation of voltage data across the total measurement period.

### B. VELOCITY PROFILES

As the UVP simultaneously captured velocity data from the Doppler shift, the pipe velocity profiles were measured to confirm the instrument’s capability to measure the flowrate. It is noted that only velocity components in the direction of the transducer are measured, and thus, the probes at 135° were used to ensure the transducers could detect the streamwise flow. As the transducer is mounted at a 135° angle, the relative inner pipe distance is 0.035 m. Transducers mounted at 90° to the flow were not used as flow velocity across the pipe is negligible, and any velocity detected using a probe mounted at 90° would be attributed to turbulence fluctuations in the pipe. Given the segregation in the horizontal arrangement, velocity profiles were only analyzed in the vertical configuration. Measurements were made with both particle sizes at two intermediate concentrations to investigate whether the suspensions affected the

accuracy of the velocity determination. Profiles are shown in dimensionless form in Fig. 11 (a) and (b) for small and large particle dispersions respectively until the middle of the pipe (which, for the probe at 135° is approximately 0.03 m). The velocity values are shown as a ratio of the peak velocity in the middle of the pipe.

For both particle systems, profiles show a marked increase in velocity at a horizontal distance of ~0.015 m, where the probe enters the suspension from the pipe wall, and peaks in the middle of the pipe at ~0.03 m, with the flattened profile shape indicative of turbulent pipe flow<sup>30</sup>. The measured profiles show consistency for both particle concentrations in each size, indicating the Doppler signal is accurately measured despite the greater attenuation in the more concentrated systems. However, the profiles were generally smoother with lower variation for the larger glass species, likely due to their enhanced scattering intensity increasing the signal to noise ratio.

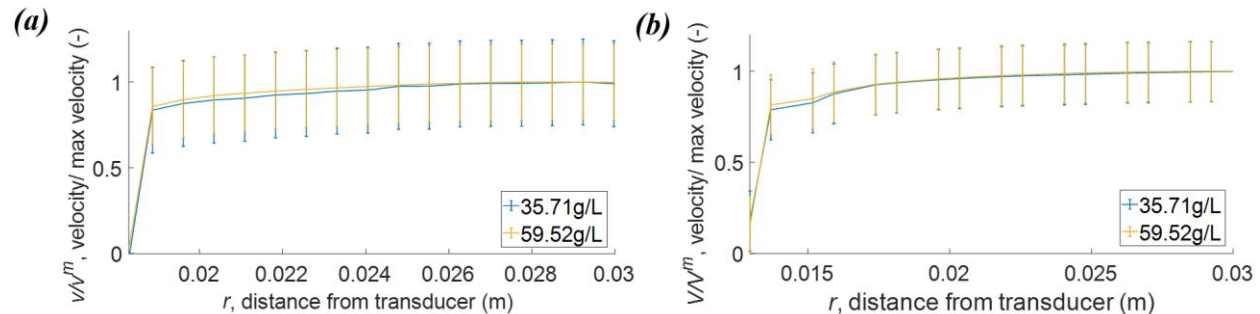


**Figure 11.** Non-dimensional velocity profiles using a vertical pipe arrangement for two concentrations of (a) small glass beads and (b) large glass beads.

## 5. CONCLUSION

Presented is an investigation into the characterization of slurry pipe flows with acoustic backscatter, using a commercial ultrasonic velocity profiler. A bespoke pipe loop system was utilized to understand the attenuation of small and large glass bead suspensions in horizontally and vertically mounted transducer holders, where the vertical pipe orientation was found to provide the most accurate attenuation and velocity profiles. The larger glass bead suspensions were found to attenuate more due to an increased rate of scattering from the larger cross-sectional area with both pipe configurations. When comparing pipe orientations, the horizontal arrangement was found to enhance attenuation producing higher coefficient values, which was likely caused by suspension segregation. This effect was especially evident with the larger glass. In comparison, attenuation coefficients from the vertical pipes correlated very closely to previous calibration values for both particle species. Simultaneous velocity profile measurement using the Doppler effect was also achieved, where, in general, profiles were as expected for highly turbulent flow. The greater scattering intensity of the larger glass produced profiles with higher signal to noise ratios.

## 6. ACKNOWLEDGEMENTS

The authors thank the Engineering and Physical Sciences Research Council (EPSRC) UK and Sellafield Ltd for funding through the Next Generation Nuclear (NGN) Centre for Doctoral Training (EP/L015390/1).

## 7. REFERENCES

- NEA. *Radiological Characterisation from a Waste and Materials End-State Perspective*. France: NEA, 2017
- Hunter, T.N., Peakall, J., and Biggs, S.R. Ultrasonic velocimetry for the *in-situ* characterisation of particulate settling and sedimentation. *Minerals Engineering*. 2011, **24**(5); doi: 10.1016/j.mineng.2010.12.003
- Hussain, S.T., Hunter, T.N., Peakall, J. and Barnes, M. Utilisation of underwater acoustic backscatter systems to characterise nuclear waste suspensions remotely. *Proceedings of Meetings on Acoustics*. 2020, **40**, 070005; doi: 10.1121/2.0001303.
- Takeda. Y. ed. *Ultrasonic Doppler Velocity Profiler for Fluid Flow*. New York: Springer Publishing, 2012.

- 
- <sup>5</sup> Hussain, S.T., Peakall, J., Barnes, M., and Hunter, T. Characterizing Flocculated Suspensions with an Ultrasonic Velocity Profiler (UVP) in Backscatter Mode. In: *IEEE IUS 2021, September 2021, Virtual*. China: IEEE, 2021; doi: 10.1109/IUS52206.2021.9593613
- <sup>6</sup> Burton, B. *Nuclear Power, Pollution and Politics*. London: Routledge, 2002.
- <sup>7</sup> Farno, E., Lester, D.R. and Eshtiaghi, N. Constitutive Modelling and Pipeline Flow of Thixotropic Viscoplastic Wastewater Sludge. *Water Research*. 2020, **184**(116126), pp1-15.
- <sup>8</sup> Mirlean, N., Baraj, B., Niencheski, L.F., Baisch, P. and Robinson, D. The Effect of Accidental Sulphuric Acid Leaking on Metal Distributions in Estuarine Sediment of Patos Lagoon. *Marine Pollution Bulletin*. 2001, **42**(11), pp1114-1117.
- <sup>9</sup> Carrera, E.V. and Paredes, M. Analysis and Evaluation of the Positioning of Autonomous Underwater Vehicles Using Acoustic Signals. *Developments and Advances in Defence and Security*. 2019, **152**(1), pp411-421.
- <sup>10</sup> Ogasawara, H., Mori, K. and Yagi, H. A Study of Acoustic Characteristics at Sea Bottom Sediment Including Organic Matter. In: *ICA. 23<sup>rd</sup> International Congress on Acoustics, 9-13 September 2019, Aachen*. Germany: ICA, 2019, pp1-5.
- <sup>11</sup> Guyson Ltd. *Glass Blast Media*. [Online]. 2020. [Accessed June 13, 2020]. Available from: <https://s3-eu-west1.amazonaws.com/resources.guyson.co.uk/product-downloads/Honite.pdf?mtime=20200117140801>.
- <sup>12</sup> Deen, W.M. *Introduction to Chemical Engineering Fluid Mechanics*. Cambridge: Cambridge University Press, 2016.
- <sup>13</sup> Ellenberger, P. *Piping and Pipeline Calculations Manual: Construction, Design Fabrication and Examination*. Oxford: Elsevier, 2014.
- <sup>14</sup> Shames, I.H. *Mechanics of fluids*. New York: McGraw-Hill, 2003.
- <sup>15</sup> Khatib, T. and Muhsen, D. *Photovoltaic Water Pumping Systems: Concept, Design, and Methods of Optimization*. Oxford: Academic Press, 2020.
- <sup>16</sup> Mazumdar, J. *Biofluid Mechanics*. Oxford: World Scientific Publishing Company, 2015.
- <sup>17</sup> Haaland, S.E. Simple and explicit formulas for the friction factor in turbulent pipe flow. *Fluid. Eng.* 1983, **105**(1), pp89-90.
- <sup>18</sup> Zagarola, M. V. and Smits, A. J. Mean-flow scaling of turbulent pipe flow. *Fluid Mech.* 1998, **373**(1), pp33-79.
- <sup>19</sup> Rice, H. P. *Transport, and deposition behaviour of model slurries in closed pipe flow Intellectual property and publication statements*. Ph.D. thesis, University of Leeds, 2013.
- <sup>20</sup> Thorne, P. D. & Meral, R. Formulations for the scattering properties of suspended sandy sediments for use in the application of acoustics to sediment transport processes. *Continental Shelf Research*. 2008, **28**(2), pp.309-317.
- <sup>21</sup> Urick, R. J., 1948. The Absorption of Sound in Suspensions of Irregular Particles. *The Journal of the Acoustical Society of America*, 20(3), pp. 283-289.
- <sup>22</sup> Kaye, G.W.C., and Laby, T.H. *Tables of Physical and Chemical Constants*. [Online]. 16<sup>th</sup> ed. Middlesex: National Physical Laboratory, 1995. [15 November 2021]. Available from: <https://web.archive.org/web/20190506031327/http://www.kayelaby.npl.co.uk/>
- <sup>23</sup> Downing, A., Thorne, P. D. & Vincent, C. E. Backscattering from a suspension in the near field of a piston transducer. *Journal of the Acoustical Society of America*. 1995, **97**(3), pp. 1614-1620.
- <sup>24</sup> Bux, J., Hunter, T.N., Paul, N., Dodds, J.M., Peakall, J. and Biggs, S.R. Characterising Nuclear Simulant Suspensions In Situ with an Acoustic Backscatter System. in: *Proceedings of the ASME International Conference on Environmental Remediation and Radioactive Waste Management, September 2013, Brussels*. Belgium: ASME, 2013, pp. 1-2.
- <sup>25</sup> Rice, H.P., Fairweather, M., Peakall, J., Hunter, T.N., Mahmoud, B. and Biggs, S.R. Measurement of particle concentration in horizontal, multiphase pipe flow using acoustic methods: Limiting concentration and the effect of attenuation. *Chemical Engineering Science*. 2015, **126**(1), pp. 745-758.
- <sup>26</sup> Biron, M. *Thermoplastics and Thermoplastic Composites*. Oxford: Elsevier, 2007.
- <sup>27</sup> MET-FLOW. *Products/ Profilers*. [Online]. 2021. [Accessed 16 April 2021]. Available from: <https://metflow.com/technology/products/uvp-duo-profilers/>
-

- 
- <sup>28</sup> Tonge, A.S., Peakall, J., Cowell, D.M.J., Freear, S., Barnes, M. and Hunter, T.N. Experimental validation of acoustic inversions for high concentration profiling of spherical particles, using broadband technology in the Rayleigh regime. *Applied Acoustics*. 2021, 180(108100); doi: 10.1016/j.apacoust.2021.108100.
- <sup>29</sup> Podesta, M. *Understanding the Properties of Matter*. Oxford: CRC Press, 2020.
- <sup>30</sup> Rennels, D.C., and Hudson, H.M. *Pipe Flow: A Practical and Comprehensive Guide*. Oxford: Wiley, 2012.